

ANALOG REALIZATIONS OF FRACTIONAL-ORDER INTEGRATORS/DIFFERENTIATORS

A Comparison

Guido Maione

DEESD, Technical University of Bari, Via de Gasperi, snc, I-74100, Taranto, Italy

Keywords: Non-integer-order operators, Fractional-order controllers, Rational approximation, Interlaced singularities.

Abstract: Non-integer differential or integral operators can be used to realize fractional-order controllers, which provide better performance than conventional PID controllers, especially if controlled plants are of non-integer-order. In many cases, fractional-order controllers are more flexible than PID and ensure robustness for high gain variations. This paper compares three different approaches to approximate fractional-order differentiators or integrators. Each approximation realizes a rational transfer function characterized by a sequence of interlaced minimum-phase zeros and stable poles. The frequency-domain comparison shows that best approximations have nearly the same zero-pole locations, even if they are obtained starting from different points of view.

1 INTRODUCTION

Originally, the investigation of integrals and derivatives of any order was a topic known as fractional calculus. In recent years, however, considerable attention has been paid to the concept of non-integer derivative and integral to model systems in various fields of science and engineering. In the research area of control theory, several authors have provided generalizations of classical controllers introducing various types of Fractional-Order Controllers (FOC). For example, the CRONE (French acronym for “*Commande Robuste d’Ordre Non Entier*”) controller (Oustaloup, 1991; Oustaloup, 1995) and Fractional-Order Proportional-Integral-Derivative (FOPID) controllers $PI^{\nu}D^{\mu}$ (Podlubny, 1999a; Podlubny, 1999b) have been recently considered. Moreover, FOC have been successfully applied in rigid robots, both for position control and for hybrid position-force-control (Tenreiro Machado and Azenha, 1998; Valerio and Sá da Costa, 2003). In general, FOC provide better performance than PID controllers, if the controlled plants are of non-integer-order. In other cases, FOC show high flexibility and can ensure high robustness for high gain variations. More particularly, in SISO systems, they can make the phase margin nearly not changing in a wide range around the gain crossover

frequency, even if high gain variations produce high changes in gain crossover frequency. Applications in mechatronics are testified by several papers (Canat and Faucher, 2005; Li and Hori, 2007; Ma and Hori, 2004a; Ma and Hori, 2004b; Ma and Hori, 2007; Melchior *et al.*, 2005).

The basic element of transfer functions of FOPID controllers is the fractional differentiator/integrator s^{ν} , with ν positive or negative real number. This operator is infinite dimensional, even if it can be approximated by finite-dimension transfer functions, whose coefficients depend on the non-integer exponent ν . A good rational approximation can be obtained by truncating the continued fractions expansion (CFE) of s^{ν} (Maione, 2006; Maione, 2008). Recently, in (Barbosa *et al.*, 2006), least-squares-based methods are used for obtaining Fractional-Order Differential Filters (FODF) approximating s^{ν} .

In this paper, a novel approach is compared to two commonly used methods to realize a rational approximation of fractional-order differentiators or integrators. These operators are the basic elements in fractional-order controllers of mechatronic systems. Section 2 revisits the three different methods systematically. Section 3 compares them in the frequency domain. Section 4 draws the conclusion with some remarks.

2 REVISITING THREE RATIONAL APPROXIMATIONS

In this section, three methods are compared. They are shortly revisited, for making a direct comparison based on transfer functions putted in the same form. All the considered realizations are known to be minimum-phase and stable, with poles interlacing zeros along the negative real half-axis of the s -plane. This property is enlightened by the form of the three transfer functions, which explicitly shows the frequencies corresponding to the alternated zeros and poles. The interlacing property is important for comparison purposes, because the position of the zero-pole pairs determines the quality of the models approximating phase and magnitude of the irrational operator $(j\omega)^\nu$. Hence, for comparison purpose, realizations are constrained to have both their zeros with minimum module and their poles with maximum module approximately equal. All the approximating transfer functions are in a factorized form, which puts in evidence the break frequencies. Then, the lowest and highest break frequencies of the proposed method are taken as reference.

2.1 The Proposed CFE Approximation

The starting point is the following continued fractions expansion (CFE):

$$(1+x)^\nu \cong b_0 + \frac{a_1}{b_1 + \frac{a_2}{b_2 + \frac{a_j}{b_j + \dots}}} \quad (1)$$

with $b_0 = b_1 = 1$, $a_1 = \nu x$ and:

$$a_j = n(n-\nu)x, \quad b_j = 2n \quad (2)$$

$$a_{j+1} = n(n+\nu)x, \quad b_{j+1} = 2n+1 \quad (3)$$

for $j = 2n$, with n natural number (Khovanskii, 1965). The analog approximation for the operator s^ν , with $0 < \nu < 1$, is given in (Maione, 2008), where $x = s-1$ is used in (1) to obtain the $(2N)$ -th convergent of the resulting CFE as approximating transfer functions:

$$\begin{aligned} \tilde{G}(\nu, s) &= \\ &= \frac{p_{N0}(\nu) s^N + p_{N1}(\nu) s^{N-1} + \dots + p_{NN}(\nu)}{q_{N0}(\nu) s^N + q_{N1}(\nu) s^{N-1} + \dots + q_{NN}(\nu)} \end{aligned} \quad (4)$$

where

$$\begin{aligned} p_{Nj}(\nu) &= q_{N,N-j}(\nu) = \\ &= (-1)^j C(N, j) (v+j+1)_{(N-j)} (v-N)_{(j)} \end{aligned} \quad (5)$$

and $C(N, j) = \frac{N!}{j!(N-j)!}$ is the binomial coefficient. Moreover:

$$(v+j+1)_{(N-j)} = (v+j+1)(v+j+2) \dots (v+N) \quad (6)$$

$$(v-N)_{(j)} = (v-N)(v-N+1) \dots (v-N+j+1) \quad (7)$$

define the Pochhammer functions with $(v-N)_{(0)} = 1$ (Spanier and Oldham, 1987). As it is easily noted, in this method the coefficients $p_{Nj}(\nu)$ and $q_{Nj}(\nu)$ are explicitly given in terms of the fractional order ν . Obviously, the positions of zeros and poles in the s -plane also depend on ν . So, $\tilde{G}(\nu, s)$ can be written in the form:

$$\tilde{G}(\nu, s) \cong k \prod_{i=1}^N \frac{1 + \frac{s}{\tilde{\omega}_{z_i}}}{1 + \frac{s}{\tilde{\omega}_{p_i}}} \quad (8)$$

As it is proved in (Maione, 2008), zeros $(-\tilde{\omega}_{z_i})$ and poles $(-\tilde{\omega}_{p_i})$ of $\tilde{G}(\nu, s)$ are all real and interlace along the negative real half-axis in the s -plane, with:

$$\tilde{\omega}_{z_1} < \tilde{\omega}_{p_1} < \tilde{\omega}_{z_2} < \tilde{\omega}_{p_2} < \dots < \tilde{\omega}_{z_N} < \tilde{\omega}_{p_N} \quad (9)$$

2.2 Oustaloup's Recursive Approximation

The CRONE controller is an integer-order frequency domain approximation of s^ν in the form:

$$G(\nu, s) \cong k \prod_{i=1}^N \frac{1 + \frac{s}{\omega_{z_i}}}{1 + \frac{s}{\omega_{p_i}}} \quad (10)$$

The gain k is adjusted so that $G(\nu, s)$ has the same crossover frequency as the ideal operator s^ν . The number N of zeros and poles of the approximating transfer function is chosen in advance. They alternate on the negative real half-axis of the s -plane so that the frequencies satisfy:

$$\omega_{z_1} < \omega_{p_1} < \omega_{z_2} < \omega_{p_2} < \dots < \omega_{z_N} < \omega_{p_N} \quad (11)$$

In this way, zeros and poles interlace on the negative real half-axis, leading to a gain which is, approximately, a linear function of the logarithm of frequency. The phase is nearly constant and approximates $\nu \pi / 2$. The parameters ω_{z_i} and ω_{p_i} are determined by placing zeros and poles as follows:

$$\alpha = \left(\frac{\omega_H}{\omega_L} \right)^{\frac{\nu}{N}}; \eta = \left(\frac{\omega_H}{\omega_L} \right)^{\frac{1-\nu}{N}}; \omega_{z_1} = \omega_L \sqrt{\eta} \quad (12)$$

$$\omega_{p_i} = \omega_{z_i} \alpha \quad i = 1, \dots, N \quad (13)$$

$$\omega_{z_{i+1}} = \omega_{p_i} \eta \quad i = 1, \dots, N-1. \quad (14)$$

The frequencies ω_L and ω_H are appropriately chosen as $\omega_L < \tilde{\omega}_{z_1}$ and $\omega_H > \tilde{\omega}_{p_N}$, so that it holds $\omega_{z_1} \cong \tilde{\omega}_{z_1}$ and $\omega_{p_N} \cong \tilde{\omega}_{p_N}$.

2.3 Matsuda's Approximation

The Matsuda's method approximates the operator s^ν from its gain ω^ν . The gain is determined at $2N+1$ frequencies $\omega_0, \omega_1, \dots, \omega_{2N}$, which are taken logarithmically spaced in the approximation interval. The interval $[\omega_0, \omega_{2N}]$ is chosen so that the lowest break frequency $\hat{\omega}_{z_1}$ and the highest break frequency $\hat{\omega}_{p_N}$ in the model satisfy: $\hat{\omega}_{z_1} \cong \tilde{\omega}_{z_1}$ and $\hat{\omega}_{p_N} \cong \tilde{\omega}_{p_N}$, respectively. Note that, usually, an odd value of N is used, so that the resulting approximation is proper. Then, the following functions are defined:

$$\begin{aligned} m_0(\omega) &= \omega^\nu; m_1(\omega) = \frac{\omega - \omega_0}{m_0(\omega) - m_0(\omega_0)}; \dots \\ \dots; m_k(\omega) &= \frac{\omega - \omega_{k-1}}{m_{k-1}(\omega) - m_{k-1}(\omega_{k-1})}; \dots \\ m_{2N}(\omega) &= \frac{\omega - \omega_{2N-1}}{m_{2N-1}(\omega) - m_{2N-1}(\omega_{2N-1})} \end{aligned} \quad (15)$$

from which the following set of parameters are obtained:

$$\alpha_0 = (\omega_0)^\nu \quad (16)$$

$$\alpha_k = \frac{\omega_k - \omega_{k-1}}{m_{k-1}(\omega_k) - m_{k-1}(\omega_{k-1})} \quad (17)$$

for $k = 1, 2, \dots, 2N$.

Using the ω_k and α_k , the CFE can be written as:

$$s^\nu \cong \alpha_0 + \frac{s - \omega_0}{\alpha_1 +} \frac{s - \omega_1}{\alpha_2 +} \frac{s - \omega_2}{\alpha_3 +} \dots \quad (18)$$

whose convergents provide the rational approximations to the irrational operator s^ν . The $(2N)$ -th convergent of (18) can be easily converted into the rational approximation, as the ratio $\hat{G}(\nu, s)$ of two polynomials with degree N . Then, the factorization of these polynomials leads to:

$$\hat{G}(\nu, s) \cong \hat{k} \prod_{i=1}^N \frac{1 + \frac{s}{\hat{\omega}_{z_i}}}{1 + \frac{s}{\hat{\omega}_{p_i}}} \quad (19)$$

Numerical experiments show that, also in this case, it holds:

$$\hat{\omega}_{z_1} < \hat{\omega}_{p_1} < \hat{\omega}_{z_2} < \hat{\omega}_{p_2} < \dots < \hat{\omega}_{z_N} < \hat{\omega}_{p_N} \quad (20)$$

3 A COMPARISON BETWEEN THREE METHODS

The approaches of the previous sections are here compared, by choosing $N = 3$ and then $N = 4$. These values are chosen to make the order of the FOC realizations as low as possible, compatibly with good performances. Figures 1, 2, 3 and 4 show the Bode plots of phase and amplitude, for the typical fractional order $\nu = 0.5$. Other values of the integer N and of ν , with $0 < \nu < 1$, can be considered. As previously stated, the approximation is performed so that $\tilde{G}(\nu, s)$, $G(\nu, s)$ and $\hat{G}(\nu, s)$ have their first zero-frequency and their last pole-frequency nearly equal. Hence, the zero-frequency $\tilde{\omega}_{z_1}$ and the pole-frequency $\tilde{\omega}_{p_3}$ or $\tilde{\omega}_{p_4}$ of $\tilde{G}(\nu, s)$ are assumed as reference. In conclusion, it must nearly hold: $\omega_{z_1} \cong \tilde{\omega}_{z_1}$, $\hat{\omega}_{z_1} \cong \tilde{\omega}_{z_1}$, $\omega_{p_3} \cong \tilde{\omega}_{p_3}$, and $\hat{\omega}_{p_3} \cong \tilde{\omega}_{p_3}$, when $N = 3$, and $\omega_{z_1} \cong \tilde{\omega}_{z_1}$, $\hat{\omega}_{z_1} \cong \tilde{\omega}_{z_1}$, $\omega_{p_4} \cong \tilde{\omega}_{p_4}$, and $\hat{\omega}_{p_4} \cong \tilde{\omega}_{p_4}$, when $N = 4$.

First, the parameters of $\tilde{G}(\nu, s)$ are determined. For $\nu = 0.5$ and $N = 3$, formula (8) gives: $\tilde{\omega}_{z_1} = 0.0521$, $\tilde{\omega}_{z_2} = 0.6360$, $\tilde{\omega}_{z_3} = 4.3119$,

$\tilde{\omega}_{p_1} = 0.2319$, $\tilde{\omega}_{p_2} = 1.5724$, $\tilde{\omega}_{p_3} = 19.1957$, and $\tilde{k} = 0.1429$. These values clearly indicate that $\tilde{G}(v, s)$ is minimum-phase, stable, with interlacing zeros and poles. Figure 1 reports the phase Bode diagram of $\arg[\tilde{G}(v, j\omega)]$ (Maione's curve).

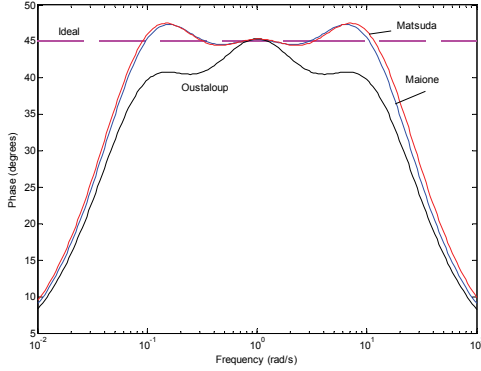


Figure 1: Phase Bode diagram for the approximations of order 3 a fractional-order differentiator, $v = 0.5$.

Now, the procedure for determining the function $G(v, s)$ is considered. With reference to (12), the interval $[\omega_L, \omega_H]$ is chosen larger than $[\tilde{\omega}_{z_1}, \tilde{\omega}_{p_3}]$. More precisely, $\omega_L = \tilde{\omega}_{z_1} \lambda_1$ and $\omega_H = \tilde{\omega}_{p_3} \lambda_2$, where λ_1 and λ_2 are coefficients to be fixed so that the Oustaloup's algorithm leads to $\omega_{z_1} \cong \tilde{\omega}_{z_1}$ and $\omega_{p_3} \cong \tilde{\omega}_{p_3}$. These coefficients are chosen by a rule of thumb. Since $\tilde{\omega}_{z_1} = 0.0521$ and $\tilde{\omega}_{p_3} = 19.1957$, simple computer experiments in MATLAB[®] show that choosing $\lambda_1 = 0.55$ and $\lambda_2 = 1.8$ yields: $\omega_{z_1} = 0.0518$, $\omega_{z_2} = 0.5509$, $\omega_{z_3} = 5.8634$, $\omega_{p_1} = 0.1688$, $\omega_{p_2} = 1.7972$, $\omega_{p_3} = 19.1293$, $k = 0.1692$. As it is noted, the constraints $\omega_{z_1} \cong \tilde{\omega}_{z_1}$ and $\omega_{p_3} \cong \tilde{\omega}_{p_3}$ are respected. In Figure 1, $\arg[G(v, j\omega)]$ is also reported (Oustaloup's curve).

Finally, for applying the Matsuda's method, the sampling frequencies are logarithmically distributed inside the approximation interval, so that it must result: $\hat{\omega}_{z_1} \cong \tilde{\omega}_{z_1}$ and $\hat{\omega}_{p_3} \cong \tilde{\omega}_{p_3}$, as requested. This result is achieved by choosing $\omega_{2N} = \lambda \tilde{\omega}_{z_1}$ and $\omega_0 = \tilde{\omega}_{p_3} / \lambda$. The parameter λ is fixed by computer experiments to $\lambda = 45$. Namely, the following breaking frequencies of $\hat{G}(v, j\omega)$ result: $\hat{\omega}_{z_1} = 0.0485$, $\hat{\omega}_{z_2} = 0.6248$, $\hat{\omega}_{z_3} = 4.5311$, $\hat{\omega}_{p_1} = 0.2207$, $\hat{\omega}_{p_2} = 1.6004$, $\hat{\omega}_{p_3} = 2.06273$, and

$\hat{k} = 0.1373$. These values show that the constraints $\hat{\omega}_{z_1} \cong \tilde{\omega}_{z_1}$ and $\hat{\omega}_{p_3} \cong \tilde{\omega}_{p_3}$ are also satisfied. As it can be easily observed, however, all the remaining frequencies and the gain of the Matsuda's model are nearly equal to those of the author's approximating transfer function. This fact is confirmed by the behaviour of $\arg[\hat{G}(v, j\omega)]$ in Figure 1 (Matsuda's curve). The Bode plot, indeed, is nearly indistinguishable from the plot of $\arg[\tilde{G}(v, j\omega)]$.

In conclusion, Figure 1 shows that $\arg[\hat{G}(v, j\omega)]$ and $\arg[\tilde{G}(v, j\omega)]$ are nearly flat and give a good approximation of $\arg[(j\omega)^v] = v\pi/2$. The plot of $\arg[\hat{G}(v, j\omega)]$ yields a slightly worst approximation. Figure 2 confirms that the magnitude plots of $\hat{G}(v, s)$ and $\tilde{G}(v, s)$ are nearly coincident. They give a better approximation of ω^v than $G(v, s)$, also in this case.

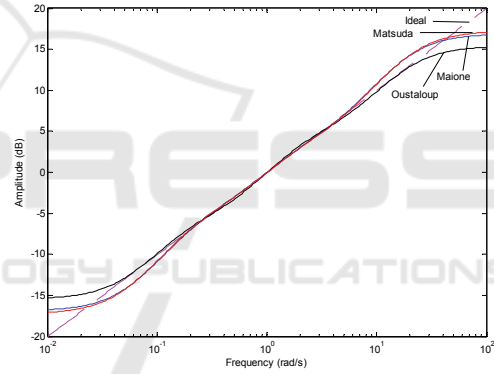


Figure 2: Amplitude Bode diagram for the approximations of order 3 of a fractional-order differentiator, $v = 0.5$.

Now, let us consider a different approximation obtained by using $N = 4$ and the same procedure.

For $v = 0.5$, formula (8) gives: $\tilde{\omega}_{z_1} = 0.0311$, $\tilde{\omega}_{z_2} = 0.3333$, $\tilde{\omega}_{z_3} = 1.4203$, $\tilde{\omega}_{z_4} = 7.5486$, $\tilde{\omega}_{p_1} = 0.1325$, $\tilde{\omega}_{p_2} = 0.7041$, $\tilde{\omega}_{p_3} = 3.0000$, $\tilde{\omega}_{p_4} = 32.1634$, and $\tilde{k} = 0.1111$. Then, $\tilde{G}(v, s)$ is minimum-phase, stable, with interlacing zeros and poles. Figure 3 shows the phase Bode diagram of $\arg[\tilde{G}(v, j\omega)]$ (Maione's curve).

For the Oustaloup's approximation, $\lambda_1 = 0.61$ and $\lambda_2 = 1.64$ yield: $\omega_{z_1} = 0.0311$, $\omega_{z_2} = 0.2261$, $\omega_{z_3} = 1.6419$, $\omega_{z_4} = 11.9237$, $\omega_{p_1} = 0.0839$, $\omega_{p_2} = 0.6093$, $\omega_{p_3} = 4.4247$, $\omega_{p_4} = 32.1323$, and $k = 0.1377$. The constraints $\omega_{z_1} \cong \tilde{\omega}_{z_1}$ and

$\omega_{p_4} \cong \tilde{\omega}_{p_4}$ are respected. In Figure 3, $arg[G(v, j\omega)]$ is also reported (Oustaloup's curve).

For the Matsuda's approximation, $\lambda = 39$ gives:
 $\hat{\omega}_{z_1} = 0.0310$, $\hat{\omega}_{z_2} = 0.3327$, $\hat{\omega}_{z_3} = 1.4211$,
 $\hat{\omega}_{z_4} = 7.5702$, $\hat{\omega}_{p_1} = 0.1321$, $\hat{\omega}_{p_2} = 0.7035$,
 $\hat{\omega}_{p_3} = 3.0055$, $\hat{\omega}_{p_4} = 32.2772$, and $\hat{k} = 0.1109$.

For $N = 4$, the frequency response of $arg[\hat{G}(v, j\omega)]$ is practically indistinguishable from that of $arg[\tilde{G}(v, j\omega)]$ (Matsuda's and Maione's curves are practically the same).

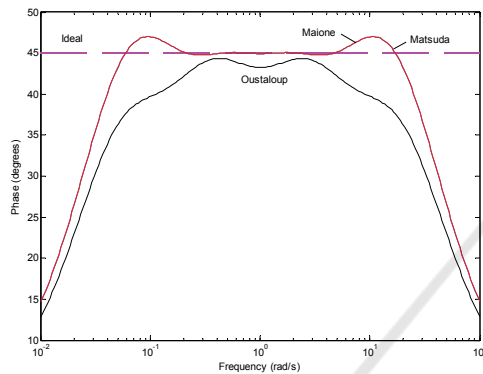


Figure 3: Phase Bode diagram for the approximations of order 4 of a fractional-order differentiator, $v = 0.5$.

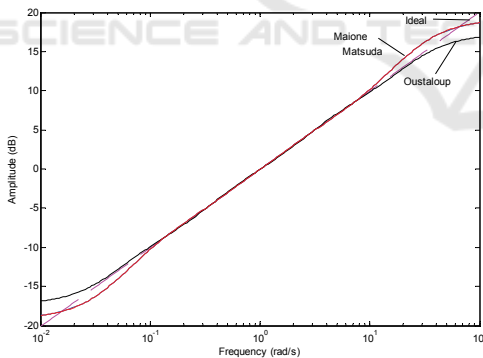


Figure 4: Amplitude Bode diagram for the approximations of order 4 of a fractional-order differentiator, $v = 0.5$.

Figure 4 confirms that the magnitude plots of $\hat{G}(v, s)$ and $\tilde{G}(v, s)$ are nearly the same and give a better approximation of ω^v than $G(v, s)$, for $N = 4$.

4 CONCLUDING REMARKS

This paper compared three different methods to approximate non-integer-order differential or

integral operators in fractional-order controllers: these methods are the author's, the Oustaloup's, and the Matsuda's, respectively. All approximations of the irrational operator s^v were realized through analog transfer functions characterized by stable poles and minimum-phase zeros. In particular, zeros and poles were interlaced along the negative real half-axis of the s -plane, and the first and last singularities were constrained to be nearly the same in all approximations. The interlacing property allowed us the comparison to find the best distribution of singularities. Namely, a frequency domain analysis of the phase diagrams showed that the author's and Matsuda's approximations outperformed the well-known by Oustaloup.

Note that all realizations were limited to the lowest order that could guarantee good performance. The better results achieved by the proposed approximation are due to a better distribution of interlaced zeros and poles. It is also interesting to note how the proposed approximation achieves nearly the same zero-pole pairs of the Matsuda's approximation, even if the starting points of the two methods are completely different.

REFERENCES

Barbosa, R.S., Tenreiro Machado, J.A., Silva, M.F., 2006. Time domain design of fractional differintegrators using least-squares. *Signal Processing*, Vol. 86, No. 10, pp. 2567-2581.

Canat, S., Faucher, J., 2005. Modeling, identification and simulation of induction machine with fractional derivative. In *Fractional Differentiation and its Applications*, Le Mehauté, A., Tenreiro Machado, J.A., Trigassou, J.C., Sabatier, J. (Eds.), Ubbooks Verlag Ed., Neusäß, Vol. 2, pp. 195-206.

Khovanskii, A.N., 1965. Continued fractions. In Lyusternik, L.A., Yanpol'skii, A.R. (Eds.): *Mathematical Analysis - Functions, Limits, Series, Continued Fractions*, chap. V, Pergamon Press. Oxford, International Series Monographs in Pure and Applied Mathematics (transl. by D. E. Brown).

Li, W., Hori, Y., 2007. Vibration suppression using single neuron-based PI fuzzy controller and fractional-order disturbance observer. *IEEE Transactions on Industrial Electronics*, Vol. 54, No. 1, pp. 117-126.

Ma, C., Hori, Y., 2004a. Backlash vibration suppression control of torsional system by novel fractional-order PID^k controller. *Transactions of IEE Japan on Industry Application*, Vol. 124, No. 3, pp. 312-317.

Ma, C., Hori, Y., 2004b. Fractional order control and its application of PI^αD controller for robust two-inertia speed control. In *Proceedings of the 4th International Power Electronics and Motion Control Conference*

- (*IPEMC 04*), Xi'an, China, 14-16 Aug. 2004, Vol. 3, pp. 1477-1482.
- Ma, C., Hori, Y., 2007. Fractional-order control: theory and applications in motion control (past and present). *IEEE Industrial Electronics Magazine*, Winter 2007, Vol. 1, No. 4, pp. 6-16.
- Maione, G., 2006. Concerning continued fractions representation of noninteger order digital differentiators. *IEEE Signal Processing Letters*, Vol. 13, No. 12, pp. 725-728.
- Maione, G., 2008. Continued fractions approximation of the impulse response of fractional order dynamic systems. *IET Control Theory & Applications*, Vol. 2, No. 7, pp. 564-572.
- Melchior, P., Sabatier, J., Duboy, D., Ferragne, H., Amagat, C., 2005. CRONE position controller for pneumatic butterfly valve controller by on-off valves. In *Fractional Differentiation and its Applications*, Le Mehauté, A., Tenreiro Machado, J.A., Trigeassou, J.C., Sabatier, J. (Eds.), Ubooks Verlag Ed., Neusäß, Vol. 3, Chap. 16, pp. 721-734.
- Oustaloup, A., 1991. *La Commande CRONE. Commande Robuste d'Ordre Non Entier*, Editions Hermès. Paris, France.
- Oustaloup, A., 1995. *La Dérivation non Entière: Théorie, Synthèse et Applications*, Editions Hermès, Serie Automatique. Paris, France.
- Podlubny, I., 1999a. *Fractional Differential Equations*, Academic Press. San Diego, CA, USA.
- Podlubny, I., 1999b. Fractional-order systems and $PI^\lambda D^\mu$ controllers. *IEEE Transactions on Automatic Control*, Vol. 44, No. 1, pp. 208-214.
- Spanier, J., Oldham, K.B., 1987. *An atlas of functions*, Hemisphere Publishing Co., New York, 1987.
- Tenreiro Machado, J.A., Azenha, A., 1998. Fractional-order hybrid control of robot manipulators. In *IEEE SMC'98, Proceedings of the 1998 IEEE International Conference on Systems, Man, and Cybernetics*, Hyatt La Jolla, San Diego (CA), USA, 11-14 Oct. 1998, pp. 788-793.
- Valerio D., Sá da Costa, J., 2003. Digital implementation of non-integer control and its application to a two link control arm. In *Proceedings of the European Control Conference*, Cambridge, UK, 1-4 Sept. 2003.